Research Article

Rapid Communications in Mass Spectrometry

Received: 21 June 2013 Revised: 6 October 2013 Accepted: 14 October 2013 Published online in Wiley Online Library

Rapid Commun. Mass Spectrom. **2014**, *28*, 77–82
(wileyonlinelibrary.com) DOI: 10.1002/rcm.6765

Is energy pooling necessary in ultraviolet matrix-assisted laser desorption/ionization?

Hou-Yu Lin[1], Botao Song[1], I-Chung Lu[1], Kuo-Tung Hsu[2], Chih-Yu Liao[2], Yin-Yu Lee[2†], Chien-Ming Tseng[3†], Yuan-Tseh Lee[1,4] and Chi-Kung Ni[1,5*]

[1]Institute of Atomic and Molecular Sciences, Academia Sinica, Taipei 10617, Taiwan
[2]National Synchrotron Radiation Research Center, Hsinchu 30076, Taiwan
[3]Department of Applied Chemistry, National Chiao Tung University, Hsinchu 30010, Taiwan
[4]Department of Chemistry, National Taiwan University, Taipei 10617, Taiwan
[5]Department of Chemistry, National Tsing Hua University, Hsinchu 30013, Taiwan

RATIONALE: Energy pooling has been suggested as the key process for generating the primary ions during ultraviolet matrix-assisted laser desorption/ionization (UV-MALDI). In previous studies, decreases in fluorescence quantum yields as laser fluence increased for 2-aminobenzoic acid, 2,5-dihydroxybenzoic acid (2,5-DHB), and 3-hydroxypicolinic acid were used as evidence of energy pooling. This work extends the research to other matrices and addresses whether energy pooling is a universal property in UV-MALDI.
METHODS: Energy pooling was investigated in a time-resolved fluorescence experiment by using a short laser pulse (355 nm, 20 ps pulse width) for excitation and a streak camera (1 ps time resolution) for fluorescence detection.
RESULTS: The excited-state lifetime of 2,5-DHB decreased with increases in laser fluence. This suggests that a reaction occurs between two excited molecules, and that energy pooling may be one of the possible reactions. However, the excited-state lifetime of 2,4,6-trihydroxyacetophenone (THAP) did not change with increases in laser fluence. The upper limit of the energy pooling rate constant for THAP is estimated to be approximately 100–500 times smaller than that of 2,5-DHB.
CONCLUSIONS: The small energy pooling rate constant for THAP indicates that the potential contribution of the energy pooling mechanism to the generation of THAP matrix primary ions should be reconsidered. Copyright © 2013 John Wiley & Sons, Ltd.

Matrix-assisted laser desorption/ionization (MALDI)[1,2] is a technique widely used for mass analysis of biomolecules. In MALDI, an analyte is mixed with a suitable matrix and placed on a sample holder. Ultraviolet (UV) laser pulses with a typical wavelength of 337 nm or 355 nm and a few nanoseconds in duration are used to strike the sample target, releasing numerous analyte and matrix molecules into the gas phase. The desorbed molecules include ions and neutrals; the ions are subsequently analyzed in a mass spectrometer. Although MALDI has been invented for more than two decades, the ionization mechanism of MALDI remains unclear.[3–10]

Several theoretical models have been proposed to explain the ion generation phenomena (protonated ions, not ions of salt) in MALDI. A popular model for generating ions is the energy pooling model proposed by Knochenmuss.[10] According to this model, molecules in a highly electronically excited singlet state (S_n) are generated through exciton hopping followed by annihilation between two molecules in the first electronically excited singlet state, (S_1-S_1energy pooling). The second annihilation between one molecule in the first electronically excited singlet state and one molecule in a highly electronically excited singlet state (S_1-S_n energy pooling), or thermal ionization from the S_n state, generates primary ions. The subsequent gas-phase ion-molecule reactions generate the ions observed in the mass spectrum.

The relationship between the first step annihilation (S_1-S_1 annihilation) and ion generation in MALDI was first proposed by Ehring *et al.*[11] They showed that fluorescence quantum yields of 2,5-dihydroxybenzoic acid (2,5-DHB) decreased as the laser fluence increased, presumably because of the S_1-S_1 annihilation processes. These annihilation processes indicate that the electronically excited states are extremely mobile and interact with each other. Exciton mobility (hopping) and S_1-S_1 annihilation have been suggested to explain the formation of ions in UV-MALDI.

A similar experiment using an excitation laser beam with a flat top profile was reported by Ludemann *et al.*[12] Both S_1-S_1 annihilation and resonant two-photon absorption are considered possible pathways of decreasing fluorescence quantum yields. Ludemann and coworkers presented a numerical model for interpreting experimental data and found that S_1-S_1 annihilation fitted the experimental data better than two-photon absorption did. The S_1-S_1 annihilation rate constants were 3.8×10^{-10} cm^3 s^{-1} for 2,5-DHB, 0.695×10^{-10} cm^3 s^{-1} for 2-aminobenzoic acid, and 6.0×10^{-10} cm^3 s^{-1} for 3-hydroxypicolinic acid.

* *Correspondence to:* C.-K. Ni, Institute of Atomic and Molecular Sciences, Academia Sinica, Taipei 10617, Taiwan. E-mail: ckni@po.iams.sinica.edu.tw

† These authors contributed equally to this work.

Knochenmuss adopted the concept of S_1-S_1 annihilation and developed a energy pooling model to quantitatively describe the ions generated in MALDI.[10] However, a recent report has highlighted that the matrix and analyte ion-to-neutral ratios (or ion yields) are not carefully distinguished in many studies.[13] The mix-up of matrix and analyte ion-to-neutral ratios results in the confusion in the discussion of the MALDI mechanism. Actually, ion-to-neutral ratios for matrices predicted using Knochenmuss's energy pooling model were approximately 10^4 times greater than many experimental measurements.[13–15] The ion-to-neutral ratios of matrix predicted from Knochenmuss's model (using 355 nm) are similar to only one report, in which the measurements were conducted using 193 nm laser pulses.[16]

At least two methods can be used to investigate S_1-S_1 annihilation. The first method involves the fluence dependence of matrix fluorescence quantum yields, as reported in previous studies. S_1-S_1 annihilation does not occur if fluorescence quantum yields do not change with variations in laser fluence. Conversely, if fluorescence quantum yields decline with increases in laser fluence, the potential reactions include (a) multi-photon absorption, (b) S_1-S_1 annihilation, or (c) other reactions involving molecules in the S_1 state. In the other words, decreases in fluorescence quantum yields at high laser fluences are not necessarily indicative of S_1-S_1 annihilation. The second method is a time-resolved fluorescence experiment using short laser pulses for excitation. The temporal evolution of fluorescence intensity is not affected by multi-photon absorption after the excitation laser pulse is complete. It provides a better measurement for reactions involving molecules in the excited state (further details are provided in the Discussion).

Because S_1-S_1 annihilation has been investigated using only three matrices (2,5-DHB, 2-aminobenzoic acid, 3-hydroxypicolinic acid), extending the research to other matrices and determining whether energy pooling is a necessary property in UV-MALDI are worthy objectives. In this work, we examined the S_1-S_1 annihilation of 2,5-DHB and 2,4,6-trihydroxyacetophenone (THAP), two common matrices used in UV-MALDI, according to the time-resolved fluorescence properties. No detectable S_1-S_1 annihilation of THAP was observed. The results showed that the upper limit of the energy pooling rate constant for THAP is 100–500 times smaller than that of 2,5-DHB. The small energy pooling rate constant for THAP indicates that the possible contribution of the energy pooling mechanism to the generation of THAP matrix primary ions should be reconsidered. The fluorescence properties of the other common UV-MALDI matrices will be reported in a separate paper to see how widespread S_1-S_1 annihilation really is.

EXPERIMENTAL

The fluorescence spectra of solid 2,5-DHB and THAP in a vacuum (1×10^{-6} Torr) were measured using a commercial spectrograph with an intensified charge-coupled device (ICCD) detector (Shamrock 303i and DH340T-18U-73 ICCD, Andor Technology). The third harmonic of an Nd:YAG laser was used for excitation (355 nm, 5 ns pulse duration, Minlite II, Continuum).

The time-resolved fluorescence intensity was determined using the third harmonic of an Nd:YAG laser (355 nm, <20 ps pulse duration, model PL2210D-1 K-P20, Ekspla, Lithuania) to excite solid samples in a vacuum (1×10^{-6} Torr), and using a streak camera (1 ps time resolution, C10910-S21, Hamamatsu Photonics K. K., Japan) to detect fluorescence. A schematic diagram of the apparatus used to measure the time-resolved fluorescence intensity is shown in Fig. 1.

The design of the rotatable sample holder was similar to that detailed in our previous report.[9] A stainless steel cylindrical sample holder (10 mm in diameter) was positioned inside the vacuum chamber, which was evacuated using a turbo molecular pump to maintain a pressure of approximately 1×10^{-6} Torr. The laser irradiation spot on the sample surface was located on the central axis of the lens. However, the rotation axis of the sample holder was offset 4 mm from the central axis of the lens. This enabled the sample surface to be changed after several laser shots by rotating the sample holder without breaking the vacuum.

All chemicals were used as purchased from Sigma-Aldrich (Sigma-Aldrich Co.) without purification (2,5-DHB 98%, THAP 98% and >99.5%). Two methods were applied to prepare the samples, the first of which was the dried-droplet method. A stock solution of 2,5-DHB or THAP was prepared by separately dissolving the corresponding compounds in a 50% acetonitrile (ACN) aqueous solution. The solution was then dropped onto a sample holder and vacuum dried. This process was repeated until the thickness of the solid sample after vacuum drying measured approximately 0.5 mm. For the second method, crystals of 2,5-DHB or THAP were packed onto the sample holder directly. The thickness of the sample was approximately 0.5–1 mm. The fluorescence time-resolved measurement showed no difference between the two sample preparation methods.

The time-resolved fluorescence intensities presented in this study were derived by averaging 3 to 5 measurements for each laser fluence. The number of measurements depended on the signal-to-noise ratio. Each measurement was based

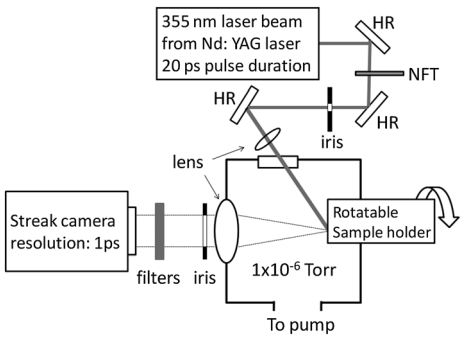

Figure 1. A schematic diagram of the time-resolved fluorescence apparatus. The filters include a dielectric coated mirror with high reflectivity for wavelengths shorter than 360 nm, and a color filter with high transmission for wavelengths longer than 385 nm. The transmittance of the filters is detailed in Fig. 3. HR: A mirror with high reflectivity at 355 nm. NFT: A step-variable metallic neutral density filter (model NDC-100S-4M, Thorlabs). The fluorescence spectra of solid 2,5-DHB and THAP in a vacuum (1×10^{-6} Torr) were measured using the same vacuum system, but the laser with 20 ps pulse duration and the streak camera detector were replaced by a laser with 5n s pulse duration and a commercial spectrograph with an intensified charge-coupled device (ICCD) detector, respectively.

on the accumulation of 10 (high laser fluence) to 200 laser shots (low laser fluence). The laser was triggered manually at a repetition rate of approximately 1 Hz. Fresh samples were used for each measurement.

RESULTS

2,5-DHB

The fluorescence spectrum of solid 2,5-DHB is shown in Fig. 2. The filters employed for time-resolved fluorescence measurements were selected according to the fluorescence spectra. The transmittance of the filters is detailed in Fig. 3.

The time-resolved fluorescence intensities obtained at various laser fluences are shown in Fig. 4. At extremely low laser fluences (0.008 and 0.016 J/m^2), the fluorescence intensity can be described using a single exponential function ($k_2 = 0$ in Eqn. (1)) with an excited state lifetime $1/k_1 = 570$ ps. The lifetime at extremely low laser fluence represents the population decays of the excited state only through photon emission, internal conversion, and intersystem crossing. As the laser fluence increases, the excited-state lifetime decreases. Thus, decreases in lifetime must be attributed to additional decay channels. The fluorescence intensity (proportional to the excited state population) can be described using a simplified equation, as recommended in a previous report:[12]

$$\frac{d[S_1(t)]}{dt} = -k_1[S_1(t)] - 2k_2[S_1(t)]^2 \quad (1)$$

The second term on the right-hand side of Eqn. (1) represents the decay caused by the reaction of two molecules in the first singlet excited state. The equation is based on the assumption that excited molecules involved in reactions do not return to the S_1 state. In other words, they no longer contribute to the fluorescence. The reaction rate constant k_2 from the fit of experimental data to Eqn. (1) ranged between $k_2 = 2 \times 10^{-11}$ and 12×10^{-11} cm^3 molecule^{-1} s^{-1} depending on the laser fluence. The values obtained under this assumption represent the lower limit of the rate constant. Details of data analysis is provided in the Discussion.

Numerous reactions involve molecules in an excited state, for example, excited state annihilation and dimerization.[17,18] However, the experimental data of this work cannot be used to determine the specific reaction that occurs between two

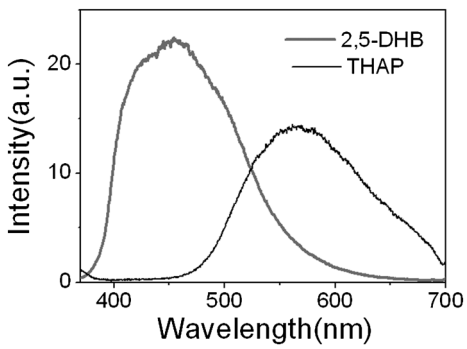

Figure 2. The fluorescence spectra of 2,5-DHB and THAP solid samples excited using 355 nm photons.

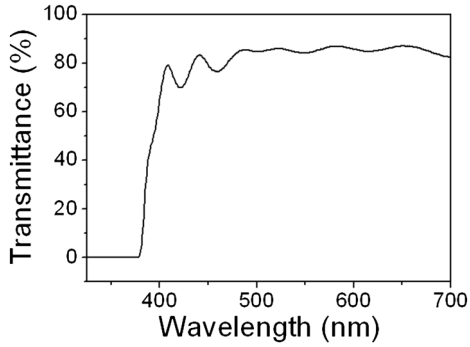

Figure 3. The transmittance of the filters employed for fluorescence measurements.

excited molecules. One potential reaction is singlet-singlet annihilation, as suggested in previous studies.[11,12]

$$S_1 + S_1 \rightarrow S_0 + S_n \quad (2)$$

If molecules in the S_n state do not return to the S_1 state through internal conversion, the situation is identical to the aforementioned assumption (excited molecules involved in reactions do not return to the S_1 state). Conversely, if molecules in the S_n state quickly relax to the S_1 state, a rate constant increased by a factor of 2 can also fit the experimental data. This can be understood by considering

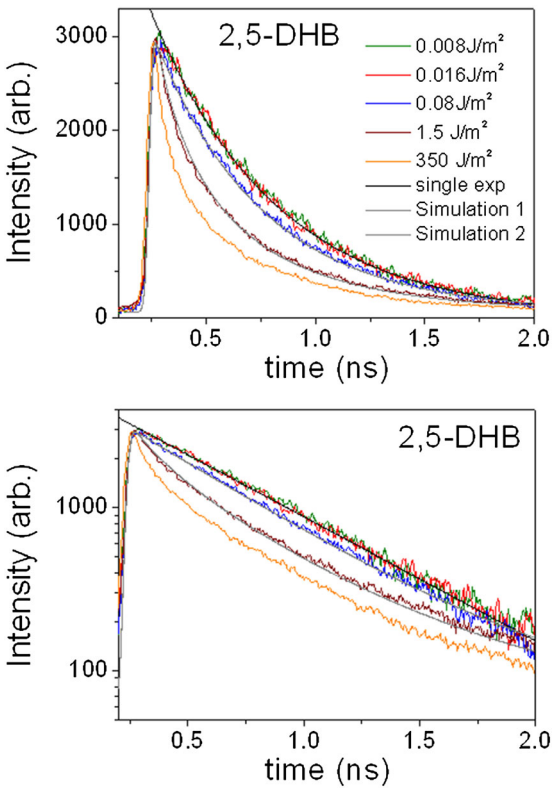

Figure 4. The time-resolved fluorescence intensity of the 2,5-DHB solid sample. Single exponential: $k_1 = 1.75 \times 10^9$ s^{-1}, $k_2 = 0$; Simulation 1: $k_1 = 2 \times 10^9$ s^{-1}, $k_2 = 2.4 \times 10^{-11}$ cm^3 molecule^{-1} s^{-1}; and Simulation 2: $k_1 = 1.8 \times 10^9$ s^{-1}, $k_2 = 1.25 \times 10^{-10}$ cm^3 molecule^{-1} s^{-1}. Both linear and log plots are shown.

that the disappearance of two molecules in the S_1 state (Eqn. (2) and no $S_n \rightarrow S_1$ relaxation) changes to a disappearance of only one molecule (Eqn. (2) followed by fast $S_n \rightarrow S_1$ relaxation).

The rate constant value obtained in this study was similar to the experimental measurement of 2,5-DHB (3.8×10^{-10} cm^3 molecule^{-1} s^{-1}) reported in a previous study.[12] The density-normalized S_1-S_1 annihilation rate constant ($k_{11} = 7 \times 10^9$ s^{-1}) was used in the simulation conducted by Knochenmuss.[10] The rate constant, k_2, in this study is related to the density normalized rate constant by $k_2 = k_{11} \times D/den$, where D represents the pooling range and den denotes the density. The value of rate constant value was $k_2 = 7.2 \times 10^{-12}$ cm^3 molecule^{-1} s^{-1} if $den = 1.44$ g/cm^3 and $D = 6$.[10] A larger pooling range[19] yields a value closer to that of experimental measurements.

THAP

Figure 5 shows that the decay curve of fluorescence intensity did not change as the laser fluence increased from 0.16 J/m^2 to 700 J/m^2. All curves can be fitted to a single exponential decay with a lifetime of 111 ps. Both THAP samples of 98% and >99.5% purity obtained from Sigma-Aldrich were examined, and no difference was observed.

DISCUSSION

Numerical simulation and comparison of the quantum yield and time-resolved fluorescence approaches

When conducting data analysis, Hillenkamp[12] found that S_1-S_1 annihilation better fitted the data compared with two-photon absorption. However, this does not mean that two-photon absorption does not contribute to decreases in fluorescence quantum yields. A superior method for measuring the contribution of S_1-S_1 annihilation without interference from two-photon absorption is to measure the time-resolved fluorescence decay by using a short laser pulse for excitation. The peak power of the short laser pulse must be identical to that of the nanosecond laser pulse used in typical MALDI experiments, to ensure that the populations in the S_1 state, $S_1(t)$, during the laser pulse are similar for both cases. The laser fluence used in this work was 0.008–350 J/m^2 for 2,5-DHB and 0.16–700 J/m^2 for THAP. The peak power at a low laser fluence, for example, 0.16 J/m^2, is similar to the typical peak power of MALDI using nanosecond laser pulses. The rate constants obtained at such a low laser fluence represent the rate constants of typical MALDI experiments.

A numerical model was developed to fit the temporal evolution of fluorescence intensity. Because fluorescence was not only collected from the surface, but also deeper in the crystals where the laser fluence was reduced because of absorption, the samples were divided into layers (each layer was 20 nm thick) for the calculations. The depth of each layer was limited to ensure that the laser fluence did not vary significantly between the top and the bottom of each layer. The temporal profile of the laser pulse intensity was described using a Gaussian function, and the pulse width

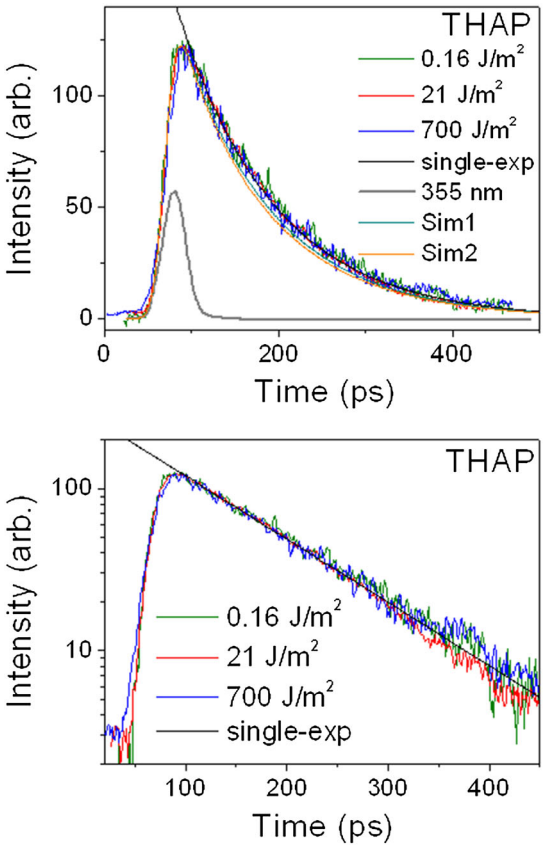

Figure 5. The time-resolved fluorescence intensity of THAP solid samples. Both linear and log plots are shown. The instrument time response function is also shown in the linear plot. The instrument time response function was derived from the measurement of 355 nm light scattered on the sample surface. In the measurement of 355 nm light, the original filters with high reflectivity for wavelengths shorter than 360 nm and high transmission for wavelengths longer than 385 nm were replaced by a narrow bandpass filter (355 ± 5 nm). Single exponential: $k_1 = 9 \times 10^9$ s^{-1}, $k_2 = 0$. Plots of Sim1 and Sim2 shows the upper limit of k_2. Sim1: $k_1 = 9\ 10^9$ s^{-1}, $k_2 = 2.4 \times 10^{-13}$ cm^3 molecule^{-1} s^{-1}; and Sim 2: $k_1 = 9\ 10^9$ s^{-1}, $k_2 = 5 \times 10^{-13}$ cm^3 molecule^{-1} s^{-1}.

was obtained from experimental measurements. Numerical simulations using the following two equations for each layer were conducted in a 1 ps time increment:

$$\frac{d[S_0(t)]}{dt} = -I(t)\alpha_0[S_0(t)] + I(t)\alpha_{0s}[S_1(t)] + k_1[S_1(t)] + k_2[S_1(t)]^2 \quad (3)$$

$$\frac{d[S_1(t)]}{dt} = I(t)\alpha_0[S_0(t)] - I(t)\alpha_{0s}[S_1(t)] - I(t)\alpha_1[S_1(t)] + I(t)\alpha_{1s}[S_n(t)] - k_1[S_1(t)] - 2k_2[S_1(t)]^2 \quad (4)$$

where α_0 and α_1 represent the absorption cross-sections from the ground state, S_0, to the first excited singlet state, S_1, and from the first excited singlet state to the higher singlet state S_n, respectively. The absorption cross-section, α_0, for 2,5-DHB is 9×10^4 cm^{-1}.[20] Additionally, α_{0s} and α_{1s} are the cross-sections of stimulated emissions from the first singlet state to the ground state, and from the higher singlet state

to the first singlet state, respectively. *I(t)* represents the laser intensity. The reaction rate constants for the first-order and second-order reactions are k_1 and k_2, respectively.

The time-dependent population in the ground state, $S_0(t)$, and the first excited state, $S_1(t)$, can be obtained by integrating Eqns. (3) and (4). Because the fluorescence intensity is proportional to the population in the first excited state, $S_1(t)$ scaled according to an arbitrary factor was used to compare experimental measurements of the time-dependent fluorescence intensity obtained in this study. The fluorescence quantum yield, *Q*, is proportional to the integration of $S_1(t)$ from the beginning of the laser pulse ($t = 0$) to the end of the fluorescence intensity decay ($t = t'$):

$$Q = C \times \int_{t=0}^{t=t'} S_1(t)dt \quad (5)$$

where *C* is the proportional constant. Fluorescence quantum yields have been used to investigate S_1-S_1 annihilation in previous studies. Because numerous excited state properties, including α_1, α_{0s}, and α_{1s}, related to multiphoton absorption and stimulated emission were not known for matrices, calculations of fluorescence quantum yields using Eqns. (3–5) include estimations of these parameters. However, these estimations contain some uncertainties. Thus, using the fluorescence quantum yield is not the optimal method for investigating S_1-S_1 annihilation. On the other hand, all terms in Eqns. (3) and (4) related to the laser intensity become zero when the laser pulse is complete (i.e., $I(t) = 0$). Equation (4) can be simplified into Eqn. (1) using a short laser pulse. This provides a superior method for investigating S_1-S_1 annihilation.

In the simulation conducted in this study, calculations of each layer were summed and compared with the experimental measurements. Because the values of α_1, α_{0s}, and α_{1s} were unknown, the numerical calculations were compared with the experimental data only after the laser pulse operation was complete.

Upper limit of k_2 for THAP

Although no contribution from the second term on the right-hand side of Eqn. (1) was observed for THAP at both low and high laser fluences, the upper limit of the rate constant k_2 for THAP can be estimated using numerical simulation. The numerical simulation, as shown in Fig. 5, suggests that the value of k_2 must be smaller than 2.4×10^{-13} cm^3 molecule^{-1} s^{-1} at a laser fluence of 700 J/m^2. This provides the upper limit of the energy pooling rate constant for THAP. The value is approximately 100 times smaller than that of 2,5-DHB at 0.08 J/m^2 ($k_2 = 2.4 \times 10^{-11}$ cm^3 molecule^{-1} s^{-1}) or 500 times smaller than that of 2,5-DHB at 1.5 J/m^2 ($k_2 = 1.25 \times 10^{-10}$ cm^3 molecule^{-1} s^{-1}). The small upper limit of k_2 for THAP suggests that energy pooling is not significant in THAP.

An alternative explanation for THAP measurement is the complete reversibility of reaction (2). In other words, once molecules are generated in the S_n state, they rapidly undergo the reverse reaction of reaction (2) (exciton fission), $S_n + S_0 \rightarrow 2S_1$. Consequently, no population decreases from S_1 because of S_1-S_1 annihilation, and fluorescence intensity do not change according to variations in laser fluence. Since all molecules generated in the S_n state return to the S_1 state, no ions are generated from the S_n state. This leads to the same inference that energy pooling is not significant to ion generation for THAP. However, if a small fraction of molecules in the S_n state do not undergo the reverse reaction, the population loss in the S_1 state may be insufficient for fluorescence-based observation. Additionally, the small fraction of molecules in the S_n state may undergo other reactions and generate ions. Consequently, the potential contribution of the energy pooling mechanism to the generation of primary MALDI ions cannot be completely excluded. However, the likelihood of this occurring is very low because no studies have reported a near-complete reversibility of reaction (2) for highly electronically excited singlet state. Fast internal conversion from S_n into a lower electronic excited state is the dominant decay channel for most molecules.

In summary, this study shows that the rate constant of the reaction between two 2,5-DHB molecules in an excited state have a similar order of magnitude as observed in previous measurements. However, the experimental data cannot be used to determine the specific reaction that occurs between two excited molecules. Energy pooling is simply one of many potential reactions. Furthermore, the small energy pooling rate constant for THAP indicates that the possible contribution of the energy pooling mechanism to the generation of THAP matrix primary ions should be reconsidered

Acknowledgements

We acknowledge the support by Thematic Research Program, Academia Sinica, Taiwan (AS-102-TP-A08) and National Science Council, Taiwan (NSC 100-2113-M-001-026-MY3).

REFERENCES

[1] K. Tanaka, H. Waki, Y. Ido, S. Akita, Y. Yoshida. Protein and polymer analyses up to m/z = 100 000 by laser ionization time-of-flight mass spectrometry. *Rapid Commun. Mass Spectrom.* **1988**, *2*, 151.

[2] M. Karas, F. Hillenkamp. Laser desorption ionization of proteins with molecular masses exceeding 10000 Daltons. *Anal. Chem.* **1988**, *60*, 2299.

[3] R. Knochenmuss, L. V. Zhigilei. What determines MALDI ion yields? A molecular dynamics study of ion loss mechanisms. *Anal. Bioanal. Chem.* **2012**, *402*, 2511.

[4] B. H. Liu, O. P. Charkin, N. Klemenko, C. W. Chen, Y.-S. Wang. Initial ionization reaction in matrix-assisted laser desorption/ionization. *J. Phys. Chem. B* **2010**, *114*, 10853.

[5] T. W. Jaskolla, M. Karas. Compelling evidence for Lucky Survivor and gas phase protonation: The unified MALDI analyte protonation mechanism. *J. Am. Soc. Mass Spectrom.* **2011**, *22*, 976.

[6] Y. J. Bae, Y. S. Shin, J. H. Moon, M. S. Kim. Degree of ionization in MALDI of peptides: Thermal explanation for the gas-phase ion formation. *J. Am. Soc. Mass Spectrom.* **2012**, *23*, 1326.

[7] Y.-H. Lai, C.-C. Wang, S.-H. Lin, Y. T. Lee, Y.-S. Wang. Solid phase thermodynamic interpretation of ion desorption in matrix-assisted laser desorption/ionization. *J. Phys. Chem. B* **2010**, *114*, 13847.

[8] S. Trimpin, B. Wang, E. D. Inutan, J. Li, C. B. Lietz, A. Harron, V. S. Pagnotti, D. Sardelis, C. N. McEwen. A mechanism for ionization of nonvolatile compounds in mass spectrometry: Considerations from MALDI and inlet ionization. *J. Am. Soc. Mass Spectrom.* **2012**, *23*, 1644.

[9] C. W. Liang, Y.-J. Lin, C. H. Lee, Y. T. Lee, C.-K. Ni, MALDI mechanism of dihydroxybenzoic acid isomers: Desorption of neutral matrix and analyte. *J. Phys. Chem. B* **2013**, *117*, 5058.
[10] R. Knochenmuss. A quantitative model of ultraviolet matrix-assisted laser desorption/ionization. *J. Mass Spectrom.* **2002**, *37*, 867.
[11] H. Ehring, B. U. R. Sundqvist. Studies of the MALDI process by luminescence spectroscopy. *J. Mass Spectrom.* **1995**, *30*, 1303.
[12] H. C. Ludemann, R. W. Redmond, F. Hillenkamp. Singlet-singlet annihilation in ultraviolet matrix-assisted laser desorption/ionization studied by fluorescence spectroscopy. *Rapid Commun. Mass Spectrom.* **2002**, *16*, 1287.
[13] M.-T. Tsai, S. Lee, I-C. Lu, K. Y. Chu, C.-W. Liang, C. H. Lee, Y. T. Lee, C.-K. Ni. Ion-to-neutral ratio of 2,5-dihydroxybenzoic acid in matrix-assisted laser desorption/ionization. *Rapid Commun. Mass Spectrom.* **2013**, *27*, 955.
[14] A. P. Quist, T. Huth-Fehre, B. U. R. Sundqvist. Total yield measurements in matrix-assisted laser desorption using a quartz crystal microbalance. *Rapid Commun. Mass Spectrom.* **1994**, *8*, 149.
[15] Y. J. Bae, Y. S. Shin, J. H. Moon, M. S. Kim. Degree of ionization in MALDI of peptides: thermal explanation for the gas-phase ion formation. *J. Am. Soc. Mass Spectrom.* **2012**, *23*, 1326.
[16] A. A. Puretzky, D. B. Geohegan. Gas-phase diagnostics and LIF-imaging of 3-hydroxypicolinic acid MALDI-matrix plumes. *Chem. Phys. Lett.* **1998**, *286*, 425.
[17] T. Hoyer, W. Tuszynski, C. Lienau. Ultrafast photo-dimerization dynamics in alpha-cyano-4-hydroxycinnamic and sinapinic acid crystals. *Chem. Phys. Lett.* **2007**, *443*, 107.
[18] T. Hoyer, W. Tuszynski, C. Lienau. Competing ultrafast photoinduced quenching reactions in cinnamic acid: peptide blends. *Phys. Chem. Chem. Phys.* **2010**, *12*, 13052.
[19] P. D. Setz, R. Knochenmuss. Exciton mobility and trapping in a MALDI matrix. *J. Phys. Chem. A* **2005**, *109*, 4030.
[20] D. A. Allwood, R. W. Dreyfus, I. K. Perera, P. E. Dyer. UV optical absorption of matrices used for matrix-assisted laser desorption ionization. *Rapid Commun. Mass Spectrom.* **1996**, *10*, 1575.